Radar Tracking System with 180nm CMOS UWB Transmitter and Small Planar Antenna Array

Alexandre M. de Oliveira[a], Marcelo B. Perotoni[b], João F. Justo[a], and Sérgio T. Kofuji[a]
[a]University of São Paulo, São Paulo, SP, Brazil; [b]Federal University of ABC, Santo André, SP, Brazil.
e-mail: {amanicoba, kofuji}@pad.lsi.usp.br; jjusto@lme.usp.br; marcelo.perotoni@ufabc.edu.br;

***Abstract* — Here it is proposed a conceptual model for geographic location of points in two dimensions, by the use of triangulation. The triangulation method here described operates on an Ultra-wideband (UWB) Timed-array module with center frequency of 4GHz. The technique consists in two arrays of planar antennas located at predetermined points, which serve as receptor for new portable UWB transmitter equipped with an omnidirectional planar antenna. The relative coordinates are then computed using proposed mathematical models. The transmitter circuit was designed using 180nm Complementary Metal Oxide Semiconductor (CMOS) – IBM (7WL_5LM_MA) process and the planar antennas were designed on FR-4 substrate. Post-Layout Spice circuit simulations show the generation of pulses with 94.5mVpp amplitudes and 514ps width. The consumption is around 677µW per pulse using a 1.8V power supply at 100MHz pulse repetition rate (PRR). 3D electromagnetic simulations were performed using CST Microwave Studio 2011, with an accuracy of less than 0.1m.**

***Keywords* — RF-microwave, Timed-array, UWB..**

I. Introduction

This paper proposes a conceptual model of a 2-dimensions tracking system for use in surveying activities in open areas, through the use of UWB antenna arrays operating at center frequency of 4GHz. An advantage of this system is that because UWB, one can determine the coordinates relative to other sources of RF UWB or narrowband emitting the signals above 3GHz. Operating as a silent and passive radar.

In order to properly operate in open-field environments, the system should have a small size, especially its antennas, which in addition to small dimensions, must operate with features such as Ultra-Wideband. In 2002, the Federal Communications Commission (FCC) approved the commercial use of the frequency band from 3.1 to 10.6 GHz [1] for UWB applications. Many researches in various fields have been performed e.g. Battlefield monitoring by micro air vehicles equipped with UWB radar [2], or the Detection of pulmonary and cardiac activities for respiratory rate and heart beat contactless monitoring [3]. These researches led to the development of this work.

The conceptual system proposed in this paper (Fig. 1) consists of two arrays of two planar UWB antennas, a single planar-type UWB omnidirectional transmitter, and the CMOS UWB transmitter (TX). The UWB receiver will not be treated in this work. The antennas, all similar, were based on the design of antenna covered elsewhere [4] with necessary adaptations, which will be addressed in the respective section.

Although it is proposed a transmitter, the system can determine the relative coordinates of any emitting source signals in any frequency that is captured by the antenna UWB.

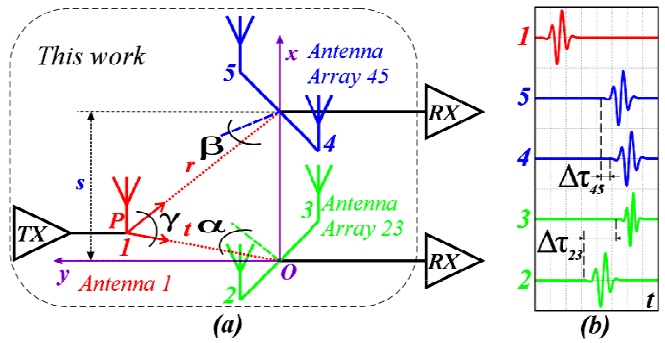

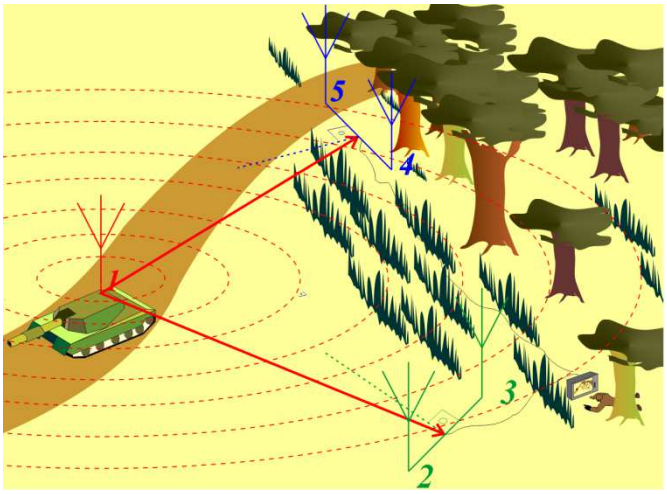

Fig. 1. (a) Illustration of the positioning system-UWB Timed Array with details of the proposed antennas and the triangulation of three different positions at different times of the transmitter; (b) signals and the respective delays that are used to calculate the angle of incidence of the signal in two antenna arrangements; (c) hypothetical scenario of application.

The work organization is as follows: in Sec II, the transmitter circuit design is presented with the Monte Carlo pos-layout Spice simulations results using LTSpice 4[5], using 180nm CMOS IBM process foundry, combined with MicroWind 3[6]; in Sec III the UWB planar antenna and the array is presented (and the model); and finally in Sec. IV are presented the simulations results of electromagnetically propagation simulation in CST MW 2011[7]. The Sec. V shows the conclusions.

II. THE NEW 5TH DERIVATIVE GAUSSIAN PULSE TRANSMITTER

In this section we present the UWB transmitter circuit and all pulse generation details.

Firstly, before designing a UWB pulse generator, must select the type of pulse that meets certain conditions [11]. Accordance with [11, 12], the Gaussian pulse can be expressed as,

$$g_{(t)} = \frac{A}{\sqrt{2\pi}\sigma} e^{\left(-\frac{t^2}{2\sigma^2}\right)} \quad (1)$$

where σ is the time variance and A is the pulse amplitude. The Gaussian pulse is a candidate for UWB transmitting because it has a wide bandwidth and no side lobes in its spectrum, but contains a DC component. According to Ref. [13] and the reasons presenteds, the fifth-order derivative Gaussian was chosen for the proposed pulse generator development. Therefore, according [13], the proposed pulse generator is

$$g^{(5)}(t) = A\left(-\frac{t^5}{\sqrt{2\pi}\sigma^{11}} + \frac{10t^3}{\sqrt{2\pi}\sigma^9} - \frac{15t}{\sqrt{2\pi}\sigma^7}\right) e^{\left(-\frac{t^2}{2\sigma^2}\right)} \quad (2)$$

A. The circuit

The circuit is composed of a triangular wave generator - a XOR gate with a delay cell in its inputs. The triangular wave generator output is then fed into a delay circuit, which feeds a pulse-shape block. In comparison to [8, 9], this proposed alternative has less elements, it is therefore less prone to yield variations and more robust. The new proposed circuit has only one triangle pulse generator in contrast to the four proposed by [8, 9]. The novel idea of the fifth-derivative Gaussian pulse generator is presented in Fig. 2.

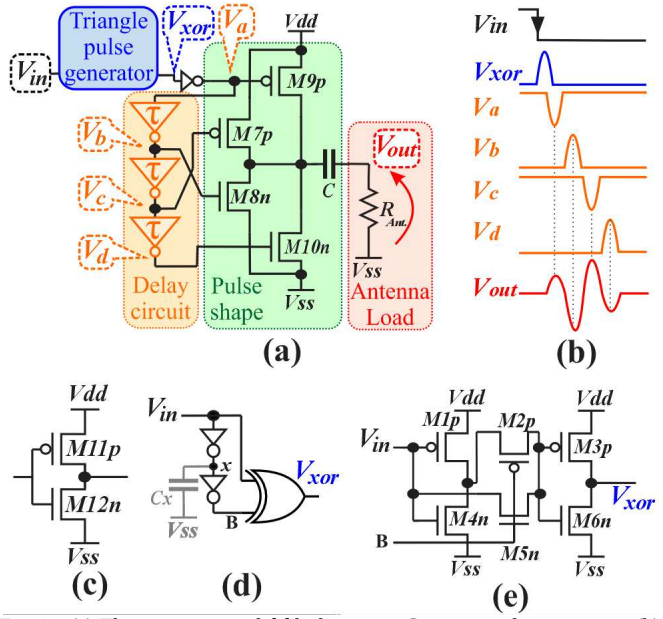

Fig. 2. (a) The new proposed fifth-derivative Gaussian pulse generator. (b) Simplified timing diagram. (c) Static invert circuit. (d) Triangle pulse generator.

The input signal (Vin) is simultaneously inserted into the input of the XOR gate adapted from ref. [10] (Fig. 2.e.) and in the delay module formed by three identical static inverters (Fig. 2.b,c). Therefore this small delay between the signals that come into two inputs of the XOR gate generates a pulse in the output triangle (***Vxor***) which is reversed by a static inverter (Fig. 2.d.). The pulse width Vxor is the sum of the delay times of the gate xor, the propagation time of two inverters and is directly linked to the parasitic capacitance of the node ***x***.

After inversion the signal (***Va***) excites the transistor M9p and is also fed into delay circuit (detail in Fig. 2.e.) which inverts and delays the signal stimulating the transistors M8n, M7p, and M10n, in that order.

The DC component of the current is blocked out by the capacitor ***C***, and also generates the ***Vout*** signal that is shaped according to the fifth-derivative Gaussian pulse illustrated in Fig.2.b.

Each subsystem of the pulse generator is described below:

1) Xor gate (triangular pulse generator):

The Xor gate circuit used in this paper is adapted on Ref. [10]. The details of the Xor gate circuit are shown in Fig.2.e.

The circuit consists of a transmission gate applying the Xor logical operator formed by three stages: a first static inverter, a transmission gate, and a second static inverter. These blocks have been designed aiming for low power consumption and high efficient operation. The first static inverter block is formed by two MOS transistors: M1p and M4n, where the dimensions of all channel lengths (***l***) are 0.18 µm and the widths (***w***) are 1.4 µm and 0.7 µm, respectively. The transmission gate block is also formed by two transistors: M2p and M5n and their widths are 1.4 µm and 0.7 µm, respectively. Finally, the second static inverter block is formed by two transistors: M3p and M6n, and the widths are 1.4 µm and 2.8 µm, respectively.

The operation details of the Xor gates follow. An operation is made between the signals of both input terminals, ***Vin*** and $\boldsymbol{Vin}_{delayed}$ (node ***B*** in Fig. 2.d.). When the first signal ***Vin*** makes a transition from "1" to "0", as the signal of the $\boldsymbol{Vin}_{delayed}$ is "1", the transition of the signal ***Vin*** is reversed in the output of second static from "0" to "1". After the delay time, the signal $\boldsymbol{Vin}_{delayed}$ changes from "1" to "0", imposing that the Xor gate output returns again to "0", and resulting in an "1" pulse every time a new pulse at the Delay input is applied shown in Fig.2 (a,b).

2) Pulse shaping stage:

The pulse shaping stage implemented two charge-pumps based on two CMOS transistors, as shown in Fig. 2.a. The gates of these transistors are excited by the pulses ***Va***, ***Vb***, ***Vc*** and ***Vd***. The charge-pump output currents are controlled and combined successively by these transistors; as a result, a fifth derivative Gaussian pulse is generated, illustrated in Fig. 2.b. The output signal magnitude ***Vout*** is controlled by output

CMOS transistors (M7-M10). The transistor sizes are chosen based on the needed amplification to shape the output UWB waveform [11]. In our design, all MOS channel lengths are 0.18µm and the widths are 1.1µm, 2.2µm, 3.6µm and 0.5µm, respectively.

3) Pulse generator simulation results:

The post-layout spice simulation results showed that the fifth-order derivative Gaussian pulse is similar to the theoretical pulse calculated, as seen in Fig. 3(a), with the simulated pulse is indicated in solid line and the normalized theoretical pulse calculated by the dotted line. The amplitude of the simulated pulse is 94,5mVpp and its pulse width has 514ps. The average power consumption of 677µW per pulse is found respectively, at input PRR's of 100MHz and 1.8V power supply.

B. Pulse transmitter simulation results

The Fig. 3.b. shows the pulse spectral density partly in accordance with the FCC mask for UWB applications.

Figure 3(b) shows the simulated power spectral density (PSD) of the proposed pulse is indicated in solid line, whereas the three-dot-dashed line shows the theoretical fifth-order Gaussian pulse PSD, alongside with the FCC mask for indoor UWB applications.

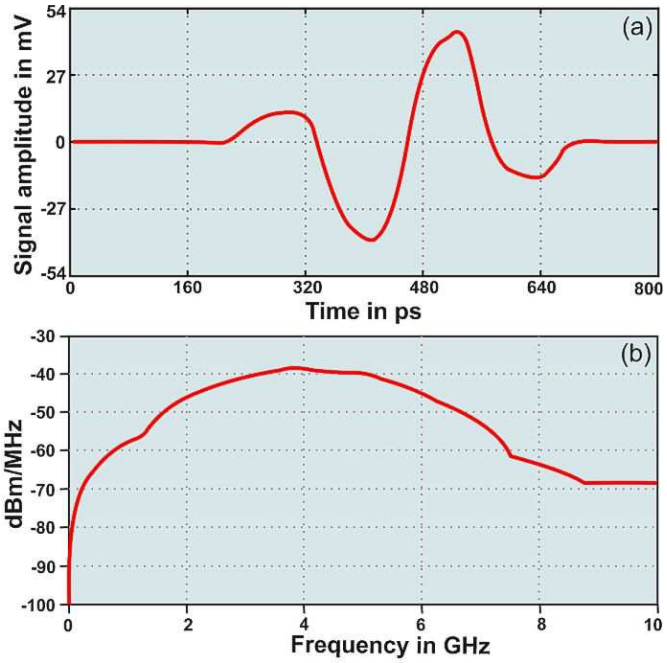

Fig. 3. (a) Simulated fifth-derivative Gaussian Pulse. (b) Spice Power Spectral Density of output pulse.

Table I presents a comparison considering this design and others reported in literature.

TABLE I. PERFORMANCE AND COMPARASION OF UWB TRANSMITTER.

Parameters	This work	[14]	[15]
pulse derivative order	5th	5th	5th
Technology	0.18µm	0.18µm	0.50µm
Power supply	1.8V	1.8V	1.8V
PRR	100MHz	100MHz	20MHz
Pulse duration	514ps	420ps	2400ps
Pulse amplitude	94.5mVpp	51mVpp	160mVpp
Power cons. per pulse.	677µW	3.6mW	1.159mW

3) Layout of the proposed UWB pulse generator

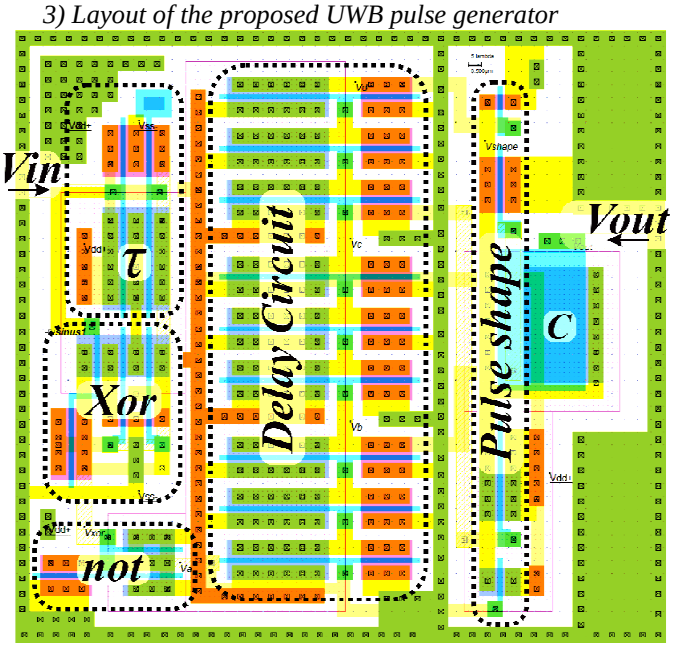

Fig. 4. Layout of pulse generator UWB without Pads.

The layout of the proposed UWB pulse generator circuit without Pads is shown in Fig. 4, where one can see, from left to right, the delay Vin signal circuit, the XOR gate (triangle pulse generator circuit), the static inverter circuit, the Delay circuit formed by three identical delay cells connected in series, each consisting of three identical inverters, the pulse shaping circuit with four MOS transistors and the C capacitor.

Around all circuits guard rings are used to minimize interference, noises and latch-up effects; because the high frequencies combined with the high miniaturization of the radio frequency CMOS circuits become more sensitive to variations in the process [16]. The whole pulse generator occupies an area of 24x25µm².

III. THE MINIATURE UWB PLANAR MONOPOLE ANTENNA AND PROPOSED ANTENNA ARRAY AND CONCEPTUAL MODEL OF TELEMETRY TRIANGULATION

In this section we present the miniature UWB planar antenna, the proposed antenna array, and the conceptual model of telemetry triangulation.

A. Characteristics in the Frequency Domain and Radiation

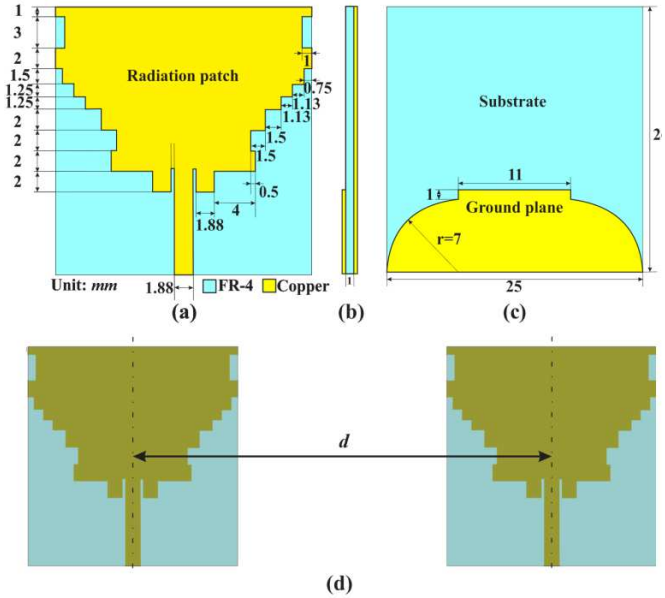

Fig. 5. Geometry of the antenna. (a) Front view. (b) Side view. (c) Back view. (d) Antenna array details.

Fig. 5. shows the geometry of the adopted staircase-bowtie planar antenna, which consists of a triangular-shaped antenna for UWB propagation, and unlike the original antenna proposed by [4], this antenna does not have a U-shaped slot.

The antenna has a total volume of 25 x 26 x 1 mm³ and is printed on both the front (radiating element and microstrip feed line) and back face (the ground plane) of a FR-4 substrate 1mm thick and with dielectric constant of 4.3.

The former U-shape was removed since simulations showed that the current geometry favored the response between 3.7 and 4.3GHz. Fig. 6 shows the Voltage Standing Wave Ratio (VSWR) plots for both antennas, for the sake of comparison.

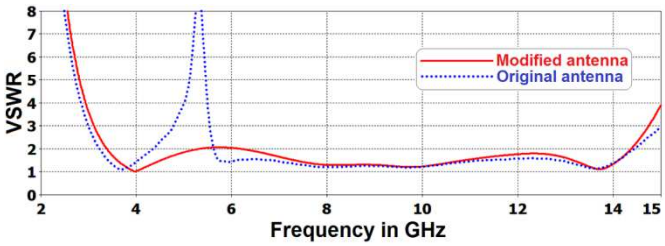

Fig. 6. Simulated VSWR with modified antenna in solid line and original antenna in doted line.

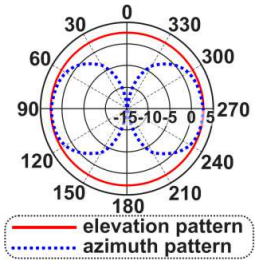

Fig. 7. Simulated radiation patterns at 4GHz with elevation in solid line and azimuth pattern represented in doted line.

The antenna radiation pattern can be see on the radiation pattern plot shown in Fig. 7.

B. Proposed antenna array and the conceptual model of telemetry triangulation

To trace the relative coordinates of the transmitter at point P (i, j) consider a fix the arrangement 23 and 45 as seen in Fig.8.

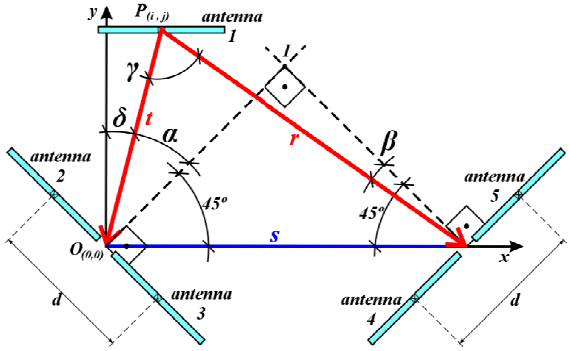

Fig. 8. Proposed distribution of antennas tracking in the Cartesian plane to the point transmitter at $P_{(i,j)}$.

It means that the origin is the center point of the arrangement 23 and the ***x*** axis that is formed by the center points of both arrays and the ***y*** axis, thus to position the transmitter in the relative position that is desired to raise the relative coordinates, considering this point as P (***i, j***) we can obtain the angle between the perpendicular line to the alignment of antennas 2 and 3 and the line formed between the central point of the array 23 and the transmitting antenna by,

$$\alpha = \left({}^{\Delta\tau_{23}}/_{|\Delta\tau_{23}|}\right) arcsin\left({}^{\Delta\tau_{23}C}/_{d}\right) {}^{180}/_{\pi} \qquad (3)$$

and the angle between the perpendicular line to the alignment of antennas 4 and 5 and the line formed between the central point of array 45 and the transmitting antenna by,

$$\beta = \left({}^{\Delta\tau_{45}}/_{|\Delta\tau_{45}|}\right) arcsin\left({}^{\Delta\tau_{45}C}/_{d}\right) {}^{180}/_{\pi} \qquad (4)$$

In both cases, $\Delta\tau_{ab}$consist in difference between $t_a$and t_b, and ***C*** is the light speed, where $C = 1/\sqrt{\varepsilon_{air}\mu_{air}} \cong 299{,}792{,}458 m/s^2$, and d is the distance between the central point of the antennas 2 in relation the 3 and 4 in relation the 5.

The relative coordinates of the transmitter $\left(P_{(i,j)}\right)$, is obtained by,

$$j = \sin(45° + \beta)\, s \frac{\sin(45°+\alpha)}{\sin(90°-\alpha-\beta)}, \qquad (5)$$

and

$$i = \sin(45° - \alpha) s \frac{\sin(45°+\beta)}{\sin(90°-\alpha-\beta)}, \qquad (6)$$

IV. Simulation Results

The simulation of the UWB transmitter with fifth-derivative Gaussian pulse generator in Spice model shows a pulse with 94.5mVpp and 514ps of pulse width, an average power consumption around 677µW per pulse using 1.8V power supply at pulse repetition rate (PRR) of 100MHz. 3D electromagnetic simulations using CST Microwave Studio 2011 showed that VSWR values below 2 for the frequency range of 3.4 to 14.4GHz, and directivity of 2.5dBi.

TABLE II. DATA OF SOME POSSIBLE SETS AND RESULTS.

Theoretical					By simulation					
s	***α***	***β***	***i***	***j***	$\Delta\tau_{23}$	$\Delta\tau_{45}$	***α***	***β***	***i***	***j***
1.0	23	-13	0.2	0.5	48	-27	22.6	-12.5	0.21	0.51
1.1	2	17	0.7	0.75	3.9	31	1.8	14.4	0.68	0.72
2.1	23	6	0.7	1.75	4.74	1.19	22.3	5.4	0.71	1.69

s, ***i***, and ***j*** in m; $\Delta\tau_{23}$ and $\Delta\tau_{45}$ in ps; ***α*** and ***β*** in degrees *(°)*.

Table II shows some possibilities for transmitter tracking with their relative coordinates obtained by the simulation where the delays were obtained $\Delta\tau_{23}$ and $\Delta\tau_{45}$, shown in the sixth and seventh columns respectively. From these delays are calculated (***i, j***) transmitter relative coordinates. Here, the first column is the distance between antenna arrays, in meters (m), the second and third column are the theoretically α and β angles, the fourth and fifth column are the theoretically coordinates of transmitter, and finally, from the eighth to eleventh, have the same parameters, however derived from the simulations. It is observed that the accuracy of this model, in the worst case, is less than 10 cm and is within expectations compared to other works of literature [17].

Table III shows a comparison between the proposed system and other different systems.

TABLE III. COMPARISON OF SYSTEMS POSITIONS.

System	**Technologie**	**Accuracy / Precision**	**Complexity / Space dimension**	**Cost**
This system	***Unidirect. UWB***	***<10cm / 99% (2m)***	***Real time response / 2D.***	***Low***
Ubisense [17]	Unidirect. UWB	15cm / 99% (0.3m)	Real time response/ 2D, 3D.	Medium
Sappire Dart[17]	Unidirect. UWB	<0.3m / 50% (0.3m)	Response frequency / 2D, 3D.	Medium
Smart LOCUS [17]	WLAN + Ultrasound	<1m / 50% (1m)	Medium / 2D	Medium
EIRIS [17]	IR + UHF + LF	<1m / 50% (1m)	Medium to High / 2D	Medium
Ekahau [17]	WALN RSSI	1m / 50% (1m)	Moderate / 2D	Low

V. Conclusions

In this paper a new method of tracking through with 180nm CMOS UWB Transmitter with Small Planar Antenna using a simulation environment integrated with Pos-Layout Spice and CST MW 2011 simulation was presented. The simulation results showed be possible to trace the relative coordinates of an 180nm CMOS UWB transmitter system of 5th-order derivative Gaussian pulse equipped with a small planar antenna, through the triangulation of the signal received by two arrays of planar UWB antennas with a precision of few centimeters. The pulses obtained shows 94.5mVpp amplitude and 514ps of pulse duration and an average power consumption around 677µW per pulse using 1.8V power supply at 100MHz of PPR.

References

[1] Federal Communication Commission, Revision of Part 15 of the Commission's Rules Regarding Ultra-Wideband Transmission Systems, adopted Feb. 2002, released Apr. 2002.

[2] R. J. Fontana, E. A. Richley, A. J. Marzullo, L. C. Beard, R. W. T. Mulloy, and E. J. Knight. An Ultra Wideband Radar for micro air vehicle applications. IEEE Conference on Ultra Wideband Systems and Technologies, 2002.

[3] A. M. De Oliveira, el al. A CMOS UWB Pulse Beamforming Transmitter with Vivaldi Array Antenna for Vital Signals Monitoring Applictions. 3rd IEEE Latin American Symposium on Circuits and Systems (LASCAS´12), EUA : IEEEXplore, 2012.

[4] Y. J. Cho, K. H. Kim, D. H. Choi, S. S. Lee, S. O. Park, A Miniature WB Planar Monopole Antenn With 5-GHz Band-Rejection Filter and the Time-Domain Characteristics. IEEE Transaction Antennas and Propagation. Vol. 54 No. 5, May 2006

[5] Linear Technology Spice (LTSpice) v.4. Linear Technology, Milpitas, CA.

[6] Microwind v.3, Dr. Etienne Sicard, Toulouse, France.

[7] Computer Simulation Technology (CST) Microwave Studio (MWS) v.2011, CST of America, Inc., Wellesley MA.

[8] H. Kim, Y. Joo, Digital Low-Power CMOS Pulse Generator for Ultra-Widband Systems. Patent No: US 7,715,502 B2. United States Patent. May 2010.

[9] H. Kim, Y. Joo, All-digital low-power CMOS pulse generator for UWB System. Electronics Letters, Vol. 40, No. 24. Nov. 2004.

[10] A. M. De Oliveira, et al. Projeto e Simulação de uma unidade Lógico-Aritmética de 8bits com tecnologia CMOS 0.35µm para aplicações didáticas. 2º Congresso Científico da Semana Tecnológica do Instituto Federal de Educação, Ciência e Tecnologia de São Paulo (CONCISTEC'11), 2011.

[11] T. A. Phan, V. Krizhanovskii, S. K. Han, S. G. Lee. 4.7pJ/pulse 7th Derivative Gaussian Pulse Generator for Impulse Radio, AUTO-ID Labs at MIT, 2008.

[12] Hongsan Sheng; Orlik, P.; Haimovich, A.M.; Cimini, L.J., Jr.; Jinyun Zhang; "On the spectral and power requirements for ultra-wideband transmission" Proceedings of IEEE International Conference on Communications (ICC´03), ISBN: 0-7803-7802-4, 2003., p.738-742.

[13] A. M. De Oliveira; et al. "A CMOS UWB Timed-Array Transmitter with a Vivaldi Antenna Array for I-Radar Applications". Proceedings of 15th SBMO - Brazilian Symposium on Microwave and Optoelectronics and 10th CBMag - Brazilian Congress of Electromagnetism (Momag 2012). ISBN: 978-85-63406-23-1. 2012.

[14] H. Xie; X. Wang; A. Wang, B. Zhao; Y. Zhou; B. Qin; H. Chen, Z. Wang; A varying pulse width 5th-derivative gaussian pulse generator for UWB transceivers in CMOS Proceedings of IEEE Radio and Wireless Symposium, 2008. ISBN: 978-1-4244-1463-5, 2008., p.171 - 174.

[15] H. Kim; Y. Joo; Fifth-derivative Gaussian pulse generator for UWB system. IEEE Radio Frequency integrated circuits (RFIC) Symposium, 2005. ISBN: 0-7803-8983-2. pp. 671-674. Aug. 2005.

[16] S. K. H. Stanley, E. S. Carlos. A 5.4 GHz Fully-Integrated Low-Noise Mixer, Journal of Integrated Circuits and Systems (JICS), Vol. 6 No. 1, p.18-29. March 2011.

[17] H. Liu; H. Darabi; P. Banerjee; J. Liu; Survey of Wireless Indoor Positioning Techniques and Systems. IEEE Transactions on Systems, Man, and Cybernetics. Vol. 37, No. 6, Nov. 2007.